Available online at www.sciencedirect.com
ScienceDirect
Mechanism and Machine Theory 43 (2008) 617–626
Mechanism and Machine Theory
www.elsevier.com/locate/mechmt

Extreme configuration bifurcation analysis and link safety length of Stewart platform

Wei-Shan Chen, Hua Chen *, Jun-Kao Liu

School of Mechatronics Engineering, Harbin Institute of Technology, Harbin 150001, PR China

Received 22 November 2006; received in revised form 12 March 2007; accepted 27 April 2007
Available online 19 June 2007

Abstract

The movement of parallel manipulator is carried out by controlling the length of links in usual condition. For a given set of motion input parameters, the Stewart platform is possibly at the states of configuration bifurcation. In order that the Stewart platform can move at will when the length of links changes in a determinate region, we discuss the problems about the manipulator configuration and link length. The extreme configuration is presented based on the idea of analyzing the movement state of parallel manipulator in link space. Sixteen kinds of extreme configurations for Stewart platform are described with the vector expressions of link lengths. In order to avoid configuration bifurcations, the bifurcation characteristics of extreme configurations are analyzed by homotopy method and static bifurcation condition. The safety length of links is solved, which makes the manipulator work safely in the safety length area of links. The relationship between the safety length of links and the structural parameters is analyzed by numerical examples.

Keywords: Extreme configuration; Bifurcation; Safety length; Stewart platform

1. Introduction

Two configurations or more of Stewart platform that can provide spatial six degree-of-freedom movement superpose possibly one another for a given set of motion input parameters called configuration bifurcation point. Configuration bifurcation is a key characteristic of singular position.

Scholars have researched much on singularity in parallel manipulator based on different point of view. Gosselin and Angeles [1] have classified singularities as singularities of the direct problem, singularities of the inverse problem and architecture singularities based on the singularity condition of Jacobian matrix. Zlatanov et al. [2] have presented a framework for the interpretation and classification of mechanism singularities. Nokleby and Podhorodeski [3] have used the properties of reciprocal screws to determine all degenerate configurations of joint-redundant manipulators. Zhao et al. [4] have studied the singularity of a spatial hybrid mechanism with screw theory. Bhattacharya et al. [5] have proposed and compared two online singularity

* Corresponding author.
E-mail address: chenhua202@126.com (H. Chen).

0094-114X/$ - see front matter
doi:10.1016/j.mechmachtheory.2007.04.010

avoidance schemes. Mlynarski and Romaniak [6] have presented a methodology of modification to analyse the kinematic properties, including the singularity of the mechanism of the loading machine. Karger [7] has discussed the singular positions and self-motions of a special class of planar parallel manipulators by giving four theorems. Shen et al. [8] have presented a finer classification and identification method for singularities in parallel mechanisms using differentiable geometry tools, and discussed the underlying physical meaning of the various singularities. Li et al. [9] have analyzed singularity locus of 3/6-Stewart platform manipulator by singularity-equivalent-mechanism. Dash et al. [10] have presented a numerical technique for path planning inside the workspace of parallel manipulators avoiding singularity. Wolf and Shoham [11] have presented a method for analyzing the type of singularity and the instantaneous behavior while in or close to a singular configuration.

Although the singularity in the parallel manipulators has been investigated to some extent, works on their bifurcation analysis at singular position are relatively few. Dasgupta et al. [12] have indicated that the manipulator loses some degrees of constraint and becomes uncontrollable at singular configurations. Innocenti et al. [13] have indicated that there is the bifurcation point at singular configuration and the manipulator will transform from one configuration to another. Wang et al. [14] have constructed the algorithm of determining all the configuration branches and bifurcation points, and investigated the configuration bifurcation characteristics in detail. These scholars have analyzed the phenomenon of configuration bifurcation in parallel manipulator at singular position. But they haven't researched farther than the motion input parameters to avoid configuration bifurcation.

In this paper, the extreme configuration is discussed based on link space, and their bifurcation characteristics are analyzed. Then, the safety length of links is solved, so as to make the manipulator avoid configuration bifurcation and unlimited by the rotation angle limit of joints and the links interference. This method is simple and convenient, and can be extended to any parallel manipulator. Because the movement of parallel manipulator is carried out by controlling the length of links in usual condition, safety length analysis is valuable in practical applications.

2. Mathematical model of Stewart platform

The Stewart platform is composed of a movable platform connected to a fixed base through six extendable links, which is shown schematically in Fig. 1. The upper extremity of each link is connected to the movable platform with a spherical joint, and six spherical joints build up two equilateral triangles. The lower extremity of each link is connected to the base with a universal joint, and six universal joints also build up two equilateral triangles. The universal joint center and the spherical joint center are denoted by b_i and p_i $(i = 1, 2, 3)$, respectively. Each link is actuated by an active prismatic joint. The Stewart platform can be described by

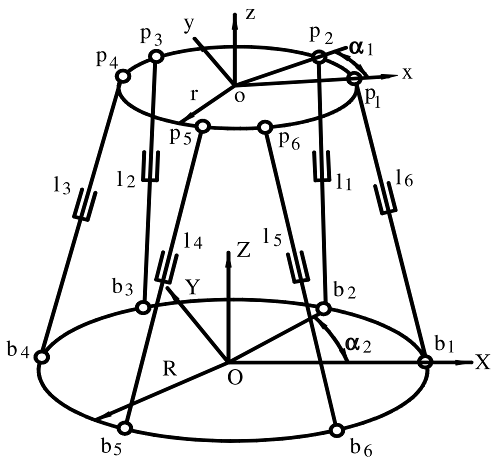

Fig. 1. Stewart platform.

six parameters which are radius parameters R and r, center angle α_1 corresponding to p_1p_2 on the movable platform, center angle α_2 corresponding to b_1b_2 on the fixed base, the maximum and minimum length of links $l_{\max}$ and $l_{\min}$. The former four parameters are usually called the structural parameters.

In addition, the joints connected on the fixed base and movable platform are passive joints for the Stewart platform driven by extendable links directly. The maximum rotation angle of passive joints and the diameter of links need to be taken into account in the kinematics analysis since they react on the normal work to Stewart manipulator.

The fixed coordinate system O-XYZ and the movable coordinate system o-xyz are established on the fixed base and the movable platforms, respectively. The origin O and o locate respectively at the centers of fixed base and movable platform, and axes Z and z are vertical respectively to fixed base and movable platform, and axes X and x pass respectively through point b_1 and p_1. The coordinates of the joints connected on the fixed base and the movable platform are denoted respectively by (x_{i0}, y_{i0}, z_{i0}) and (x_i, y_i, z_i) $(i = 1, 2, \cdots, 6)$, and the center coordinates of movable platform is represented by (x_0, y_0, z_0), and the orientation is represented by $(\theta_x, \theta_y, \theta_z)$ that is the rotation angles of the movable platform around the fixed coordinate axes. The configuration of Stewart platform manipulator can be expressed by the position and orientation of the movable platform. Suppose the length vector of the links is $\boldsymbol{L} = [l_1, l_2, l_3, l_4, l_5, l_6]^{\mathrm{T}}$, we describe the position and orientation of the movable platform by the center coordinate (x_0, y_0, z_0) of the movable platform and the two spherical joints' coordinates (x_1, y_1, z_1), (x_2, y_2, z_2) based on the expressions given by [15].

According to the constraint condition of links' lengths and the geometry relation of the movable platform, the constraint equation set with nine dimensions is simply noted as

$$\begin{cases} \boldsymbol{F}(\boldsymbol{x}, \boldsymbol{L}) = 0 \\ \boldsymbol{x} = [x_0, y_0, z_0, x_1, y_1, z_1, x_2, y_2, z_2]^{\mathrm{T}} \\ \boldsymbol{L} = [l_1, l_2, l_3, l_4, l_5, l_6]^{\mathrm{T}} \end{cases} \tag{1}$$

The variable $\boldsymbol{x}$ in the above equation can be calculated by numerical method, so as to obtain the position coordinate (x_0, y_0, z_0) of the movable platform's center. The orientation of the movable platform is

$$\theta_x = \tan^{-1}\frac{m_z}{n_z}, \quad \theta_y = \tan^{-1}\frac{-(z_1 - z_0)}{\sqrt{(x_1 - x_0)^2 + (y_1 - y_0)^2}}, \quad \theta_z = \tan^{-1}\frac{y_1 - y_0}{x_1 - x_0} \tag{2}$$

where m_z and n_z are the functions about $x_0, y_0, z_0, x_1, y_1, z_1, x_2, y_2, z_2$.

3. Extreme configuration analysis

3.1. Kinds of extreme configurations

The workspace of Stewart platform is restricted by some factors such as the structural parameters of movable platform, the maximum and minimum length of links, the maximum rotation angle of passive joints and the diameter of links. When the structural parameters, the configuration of passive joints and the diameter of links are certain, the workspace is decided only by the lengths of six links. We define the concept about extreme configuration based on the link space to this question: extreme configuration is a kind of manipulator configuration whose every link is on the state of maximum or minimum length. On this condition, we suppose that the position and orientation of movable platform is only restricted by the constraint of link length, the rotation angle limit of joints and the interference between any two links are not considered.

Stewart platform has 16 kinds of extreme configurations listed in Table 1. In this table, the vector expression represents the state of six links (0 – minimum length, 1 – maximum length), and the extreme configuration figured in Table 1 is only one kind of situation because that it will be another while initial configuration is different. Other extreme configuration corresponding to link's extreme state will superposes with one of these 16 kinds of extreme configurations because the manipulator is symmetrical.

Table 1
Sixteen kinds of extreme configurations

No.	Vector expression	Extreme configuration	Links' number of maximum length
1	[0 0 0 0 0 0]	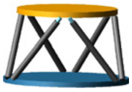	0
2	[0 0 0 0 0 1]	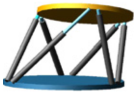	1
3	[0 0 0 0 1 1]	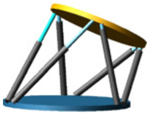	2
4	[0 0 0 1 0 1]	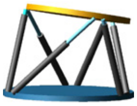	2
5	[0 0 0 1 1 0]		2
6	[0 0 1 0 0 1]	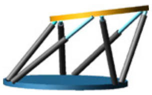	2
7	[0 0 0 1 1 1]	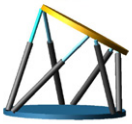	3
8	[0 0 1 0 1 1]	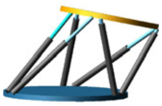	3
9	[0 1 0 1 0 1]		3
10	[0 1 0 1 1 0]		3
11	[0 0 1 1 1 1]		4

Table 1 (*continued*)

No.	Vector expression	Extreme configuration	Links' number of maximum length
12	[0 1 0 1 1 1]		4
13	[0 1 1 0 1 1]	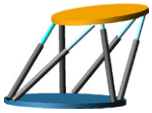	4
14	[0 1 1 1 1 0]		4
15	[0 1 1 1 1 1]		5
16	[1 1 1 1 1 1]		6

3.2. Solving forward kinematics problem of initial configuration based on homotopy method

The problem about mechanism often is come down to nonlinear polynomial algebra system. Numerical iterative method can be used to solve the nonlinear polynomial algebra system. The main problem of traditional numerical iterative method is selecting iterative initial value. Homotopy method presented in the 70th decade of the 20th century is an effective numerical iterative method. It has some advantages such as depending little on iterative initial value, strong astringency and solving reliably all or isolated solutions of nonlinear equation set. So homotopy method is paid much attention on the domain of engineering technology [16–18].

On initial situation, supposing every link is on the state of minimum length, the length vector of links is $\boldsymbol{L}_0 = [l_{\min}, l_{\min}, l_{\min}, l_{\min}, l_{\min}, l_{\min}]^{\mathrm{T}}$. We will find out all possible initial configurations of manipulator using homotopy iterative method.

Construct a homotopy function $\boldsymbol{H}(\boldsymbol{x},\boldsymbol{L}_0,t)$ including homotopy parameter $t \in [0,1]$ for constraint equation (1). The homotopy function is

$$\boldsymbol{H}(\boldsymbol{x},\boldsymbol{L}_0,t) = t\boldsymbol{F}(\boldsymbol{x},\boldsymbol{L}_0) + (1-t)\gamma\boldsymbol{G}(\boldsymbol{x},\boldsymbol{L}_0) = 0 \tag{3}$$

where γ is an appropriate nonzero complex constant with nonzero virtual component; $\boldsymbol{G}(\boldsymbol{x},\boldsymbol{L}_0)$ is the initial equation set whose solution set has been known, and we let

$$\boldsymbol{G}(\boldsymbol{x},\boldsymbol{L}_0) = [x_0^2-1, y_0^2-1, z_0^2-1, x_1^2-1, y_1^2-1, z_1^2-1, x_2^2-1, y_2^2-1, z_2^2-1]^{\mathrm{T}}$$

Thus, the values of position components of movable platform are obtained by tracing the solution curves of the homotopy function equation (3). And the values of orientation components are obtained using Eq. (2). The structure parameters of the Stewart platform are: $R = 2$ m, $r = 1.5$ m, $\alpha_1 = 90°$, $\alpha_2 = 20°$, $l_{\min} = 2$ m. All eight real solutions are obtained and listed in Table 2 by tracing 512 homotopy paths, that is there is eight

Table 2
All real solutions of initial configurations

No.	x_0 (m)	y_0 (m)	z_0 (m)	θ_x (°)	θ_y (°)	θ_z (°)
1	0	0	1.6325	0	0	−35
2	0	0	−1.6325	0	0	−35
3	−0.50975	0.60728	0.72361	31.865	63.09	−15.12
4	−0.50975	0.60728	−0.72361	−31.865	−63.09	−15.12
5	−0.27113	−0.74494	0.72361	−66.681	−13.824	−25.88
6	−0.27113	−0.74494	−0.72361	66.681	13.824	−25.88
7	0.7807	0.13766	0.72361	59.509	−40.752	−58.974
8	0.7807	0.13766	−0.72361	−59.509	40.752	−58.974

kinds of assembled configuration. In this table, the 1st configuration is usually employed, that is the horizontal movable platform locates over the fixed base, and the coordinates along x and y of movable platform's center are all zero.

3.3. Extreme configuration bifurcation analysis

On initial situation, we suppose that every link is on the state of minimum length, that is the manipulator is on the state of the 1st extreme configuration. Varying with the length variables of links, the manipulator locates on the state of other 15 kinds of extreme configuration. On every state of extreme configuration, in order to analyze the change of status variable $\boldsymbol{x}$ when the length of stretched-out links increase constantly from the minimum value, we select the length variable of stretched-out links μ as configuration bifurcation parameter. For example with the 2nd extreme configuration, we introduce the method of extreme configuration bifurcation analysis in the following, and then, give the results of other extreme configuration bifurcation analysis.

On the 2nd extreme configuration state, the length vector of links is $\boldsymbol{L} = [l_{\min}, l_{\min}, l_{\min}, l_{\min}, l_{\min}, \mu]^{\mathrm{T}}$. Thus, the bifurcation equation is

$$\begin{cases} \boldsymbol{F}(\boldsymbol{x}, \boldsymbol{L}) = 0 \\ \boldsymbol{x} = [x_0, y_0, z_0, x_1, y_1, z_1, x_2, y_2, z_2]^{\mathrm{T}} \\ \boldsymbol{L} = [l_{\min}, l_{\min}, l_{\min}, l_{\min}, l_{\min}, \mu]^{\mathrm{T}} \end{cases} \tag{4}$$

In order to analyze the variable $\boldsymbol{x}$ corresponding with the variation of the bifurcation parameter μ, the new configuration needs to be calculated while the bifurcation parameter changes from $\mu_0 = l_{\min}$ to μ. So, letting the equation set $\boldsymbol{F}(\boldsymbol{x}, \boldsymbol{L}_0) = 0$ of manipulator's initial state as initial equation set whose solution set has been obtained in last section, we construct the following homotopy equation set

$$\boldsymbol{H}(\boldsymbol{x}, \boldsymbol{L}, t) = t\boldsymbol{F}(\boldsymbol{x}, \boldsymbol{L}) + (1 - t)\gamma\boldsymbol{F}(\boldsymbol{x}, \boldsymbol{L}_0) = 0 \tag{5}$$

Because of getting rid of all emanative paths, the computing efficiency of this kind of method for constructing homotopy equation set is very high when the polynomial equation set having same structure and differ coefficients is solved. Beginning from all solutions of initial equation set, and tracing all homotopy paths, we can obtain all solutions of $\boldsymbol{F}(\boldsymbol{x}, \boldsymbol{L}) = 0$, which are all configurations whose length of stretched-out links is μ. The solution curves are shown in Fig. 2.

The singular points on the curves are obtained by the judgment condition

$$\begin{cases} \boldsymbol{F}(\boldsymbol{x}, \boldsymbol{L}) = 0 \\ \det(\boldsymbol{F}_x(\boldsymbol{x}, \boldsymbol{L})) = 0 \end{cases} \tag{6}$$

where $\boldsymbol{F}_x(\boldsymbol{x}, \boldsymbol{L})$ is a 9×9 matrix that is the one-order derivative of $\boldsymbol{F}$ by every element of $\boldsymbol{x}$. From Eq. (6), the four singular points are obtained and listed in Table 3.

As shown in Fig. 2 and Table 3, beginning from initial configurations, when increasing the length of stretched-out link μ, the 2nd extreme configuration varies with eight configuration branches to singular point,

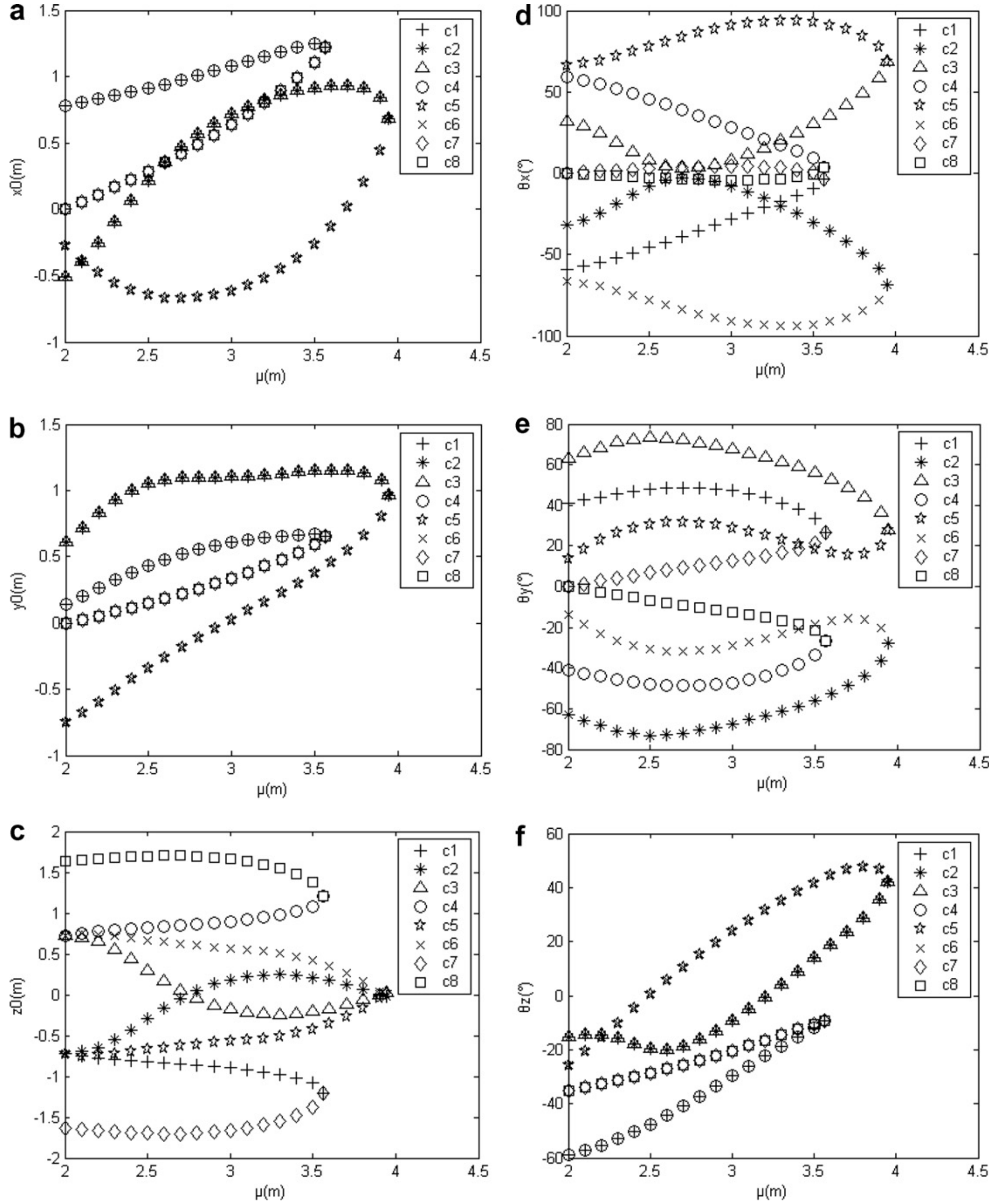

Fig. 2. The 2nd extreme configuration bifurcation graph. Configuration bifurcation branch of component x_0 (a), y_0 (b), z_0 (c), θ_x (d), θ_y (e) and θ_z (f).

Table 3
Singular points of the 2nd extreme configuration

Singular points	μ (m)	x_0 (m)	y_0 (m)	z_0 (m)	θ_x (°)	θ_y (°)	θ_z (°)
1	3.5635	1.2175	0.65089	1.2086	3.8252	−26.442	−9.4771
2	3.5635	1.2175	0.65089	−1.2086	−3.8252	26.442	−9.4771
3	3.9453	0.68616	0.96312	0.02359	68.725	27.723	42.136
4	3.9453	0.68616	0.96312	−0.02359	−68.725	−27.723	42.136

Table 4
Singular points of all extreme configurations

Extreme configuration	μ (m)	x_0 (m)	y_0 (m)	z_0 (m)	θ_x (°)	θ_y (°)	θ_z (°)
2	3.5635	1.2175	0.6509	1.2086	3.83	−26.44	−9.48
3	5.128	0.7483	2.056	−0.8618	−150.02	−7.63	−7.04
4	3.422	1.0287	−0.6048	1.3482	6.72	−23.77	15.07
5	4.4567	1.2796	0.2256	1.228	−165.03	14.48	−123.09
6	2.9793	1.4678	0.2588	1.3552	18.34	−17.47	−37.84
7	3.9624	0.6777	−0.0139	2.3957	−55.20	15.51	3.84
8	3.4632	1.4629	1.6207	0.9264	−8.08	−40.07	−58.19
9	3.2989	0	0	1.0915	0	0	55
10	3.255	−0.6561	0.7595	1.8137	−37.82	53.64	−28.86
11	4.1396	3.0905	0.5449	0.8578	−38.91	32.13	−46.62
12	3.5033	−0.1345	0.7813	1.812	−31.59	42.89	32.99
13	3.7988	0.3510	0.9645	2.2219	119.29	13.15	−12.73
14	3.1264	−0.5269	0.6280	2.2598	14.77	43.57	−29.07
15	3.5825	0.7562	1.5074	2.392	10.95	48.89	1.32

where two kinds of configuration branches overlap. When decreasing the length of stretched-out link μ comes very close to a singular point, the movable platform can give out the output with two kinds of configurations. Therefore, the output of the movable platform is uncertain because of configuration bifurcation.

We analyze the singular point of extreme configuration when the initial assembled configuration is the 1st configuration in Table 2. We can know that the singular point corresponding to the 2nd extreme configuration is the 1st singular point in Table 3, which shows that the 2nd extreme configuration is singular when the length of stretched-out links achieves at 3.5635 m under this kind of initial assembled configuration. We obtain the singular points of other extreme configurations on this kind of initial assembled configuration using above method, which are listed in Table 4. The 16th kind of extreme configuration has not singular point.

It can be found that the value μ of singular point of the 6th extreme configuration is the minimum. Under this kind of extreme configuration, when the rotation angle limit of joints and the interference between any two links are not considered, the manipulator cannot work normally unless the length of links is less than 2.9793 m. So, the maximum length of links $l_{\max}$ should be less than this value so that the manipulator can work normally.

4. Safety length of links

4.1. Maximum safety length

In order to avoid configuration bifurcations on bifurcation points, when the minimum length $l_{\min}$ is known, the maximum safety length $l_{\max}$ is limited by solving the bifurcation points of extreme configurations. Supposing the minimum value of variable μ in bifurcation points of all extreme configurations is μ^*, when the given controllable precision to the length parameter of links is ε, the maximum safety length of links should satisfy

$$l_{\max} = \mu^* - \varepsilon \tag{7}$$

Thus, the safety travel of links will be

$$h = l_{\max} - l_{\min} \tag{8}$$

This is valuable in practical mechanism optimization. If the mechanism with the length area [$l_{\min}$, $l_{\max}$] of links can satisfy the workspace required, the Stewart platform working normally should not present configuration bifurcations when the length of six links are arbitrary values among the length area. Thus optimal design of parallel manipulator is achieved.

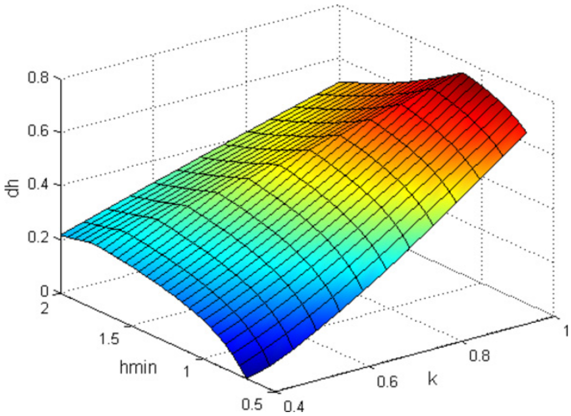

Fig. 3. Relation between$k$, $h_{\min}$ and dh.

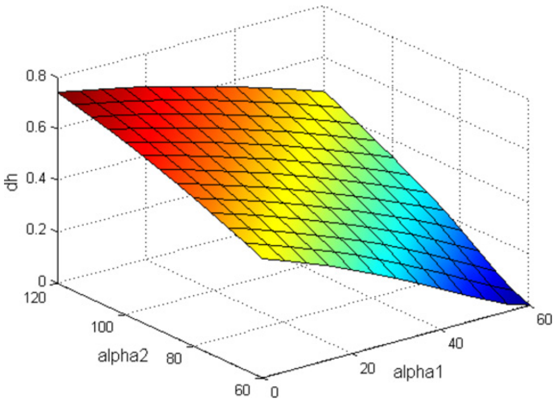

Fig. 4. Relation between α_1, α_2 and dh.

4.2. Relation between structure parameters and safety travel

Taking the radius R of the fixed base as nondimensional scale, we carry out the nondimensional treatments as $k = r/R$, $h_{\min} = l_{\min}/R$, $\mathrm{d}h = h/R$. The bigger the value of dh, bigger the safety travel is to a determinate mechanism.

We can obtain the relation curve about k, $h_{\min}$ and dh after giving center angles α_1 and α_2. Several relation curves about k, $h_{\min}$ and dh with different α_1 and α_2 are calculated, which have close shape shown as Fig. 3. As shown in this figure, the safety travel is longer when k closes to 1, i.e., the radius of fixed base is closed to the radius of movable platform.

Fig. 4 shows the variation of safety length corresponding the center angles α_1 and α_2. In this figure, with the given k and $h_{\min}$, we can find that the safety travel descends with α_1 and increases with α_2. The bigger the value of α_1 and smaller the value of α_2, longer the safety travel is. Of course, the two center angles are restricted by the mechanism structure in practical design.

5. Conclusion

Based on extreme configuration bifurcation analysis in link space, the safety length of links can be obtained by solving the bifurcation point in configuration curve beginning with the position and orientation of a given initial assembled configuration. By restricting the length of links, the presented analysis method of safety length of links makes the configuration bifurcations should not occur. Because the movement of parallel manipulator is carried out by controlling the length of links in usual condition, safety length analysis is valuable in practical applications.

References

[1] C. Gosselin, J. Angeles, Singularity analysis of closed-loop kinematic chains, IEEE Trans. Robot. Automat. 6 (3) (1990) 281–290.

[2] D. Zlatanov, R.G. Fenton, B. Benhabib, A unifying framework for classification and interpretation of mechanism singularities, J. Mech. Design 117 (4) (1995) 566–572.

[3] S.B. Nokleby, R.P. Podhorodeski, Reciprocity-based resolution of velocity degeneracies (singularities) for redundant manipulators, Mech. Mach. Theory 36 (3) (2001) 397–409.

[4] J.S. Zhao, K. Zhou, Z.J. Feng, Z.Y. Tan, The singularity study of spatial hybrid mechanisms based on screw theory, Adv. Manuf. Technol. 25 (9–10) (2005) 1053–1059.

[5] S. Bhattacharya, H. Hatwal, A. Ghosh, Comparison of an exact and an approximate methodology of singularity avoidance in platform type parallel manipulators, Mech. Mach. Theory 33 (7) (1998) 965–974.

[6] T. Mlynarski, K. Romaniak, The methodization of examination of the mechanisms of high structural complexity, Mech. Mach. Theory 36 (6) (2001) 709–715.

[7] A. Karger, Singularities and self-motions of equiform platforms, Mech. Mach. Theory 36 (7) (2001) 801–815.

[8] H. Shen, X.Z. Wu, G.F. Liu, Z.X. Li, Classification and identification of singularities of parallel mechanism, Chin. J. Mech. Eng. 40 (4) (2004) 30–35 (in Chinese).

[9] Y.W. Li, Z. Huang, L.H. Chen, Singular loci analysis of 3/6-Stewart manipulator by singularity-equivalent-mechanism, in: The IEEE International Conference on Robotics and Automation, Taipei, Taiwan, 2003, pp. 1881–1886.

[10] A.K. Dash, I-M. Chen, S.H. Yeo, G. Yang, Singularity-free path planning of parallel manipulators using clustering algorithm and line geometry, in: The IEEE International Conference on Robotics and Automation, Taipei, Taiwan, 2003, pp. 761–766.

[11] A. Wolf, M. Shoham, Investigation of parallel manipulators using linear complex approximation, J. Mech. Des. 125 (2003) 564–572.

[12] B. Dasgupta, T. Mruthyunjaya, The Stewart platform manipulator: a review, Mech. Mach. Theory 35 (2000) 15–40.

[13] C. Innocenti, V.P. Castelli, Singularity-free evolution from one configuration to another in serial and fully-parallel manipulators, Trans. of ASME, J. Mech. Des. 120 (3) (1998) 73–79.

[14] Y.X. Wang, Y.M. Wang, Configuration bifurcations analysis of six degree-of-freedom symmetrical Stewart parallel mechanisms, Trans. of ASME, J. Mech. Des. 127 (1) (2005) 70–77.

[15] Y.X. Wang, Y.M. Wang, Y.S. Chen, Z. Huang, Research on loss of controllability of Stewart parallel mechanism at bifurcation points, Chin. J. Mech. Eng. 41 (7) (2005) 40–44 (in Chinese).

[16] Z. Mu, K. Kazerounian, A real parameter continuation method for complete solution of forward position analysis of the general Stewart, J. Mech. Des. 124 (2) (2002) 236–244.

[17] G. Wang, X. Wang, Forward displacement analysis of two classes of Stewart platform using one unified mathematical model, Syst. Contr: Theory Appl. (2000) 65–70.

[18] E. Wolbrecht, H. Su, A. Perez, J.M. McCarthy, Geometric design of symmetric 3-rrs constrained parallel platforms, Proc. ASME Dyn. Syst. Contr. Div. 73 (2) (2004) 1059–1064.